Rapid turnover of sex chromosomes likely drives speciation in Neotropical armored catfish *Harttia* (Siluriformes, Loricariidae)

Francisco de Menezes Cavalcante Sassi[1, 2, 3, *], Fernando Henrique Santos de Souza[2, 4], Foyez Shams[3], Manolo Fernandez Perez[5], Tariq Ezaz[3], Geize Aparecida Deon[2, 3], Luohao Xu[1], Marcelo de Bello Cioffi[2]

[1]Key Laboratory of Aquatic Science of Chongqing, College of Life Sciences, Southwest University, Chongqing 400715, China.
[2]Laboratory of Evolutionary Cytogenetics, Universidade Federal de São Carlos, São Carlos – SP 13565-905, Brazil.
[3]Institute for Applied Ecology, University of Canberra, Canberra – ACT 2617, Australia.
[4]Department of Zoology, Faculty of Science, Charles University, Prague 1594, Czech Republic.
[5]Real Jardín Botánico – RJB-CSIC, Madrid 28014, Spain.

Abstract: The genus *Harttia* represents an important repository of multiple sex chromosomes, as they are found in more than a quarter of its valid species, exhibiting distinct degrees of heteromorphism. However, little is known about the evolution of these systems from a molecular perspective. In this study, we generated DArTseq data for 17 species of *Harttia* and one outgroup species (*Farlowella* sp.) to investigate the genomic architecture underlying sex chromosome evolution in this highly dynamic genus. The time-calibrated phylogeny based on 1,381 SNPs revealed three well-supported clades, with divergence between clades occurring approximately 6 to 10 million years ago (Mya), coinciding with the formation of the Amazon River and several other river capture events in South America. The reconstruction of ancestral areas and karyotype, combined with the identification of shared and specific sex-linked markers, suggests that the *Harttia* ancestor occupied either the South and Southeast Atlantic drainages or the Eastern Amazon, with a karyotype of 2n = 58 and a homomorphic XY system. Our findings indicate the recent and independent emergence of two distinct multiple sex chromosome systems at ~5 Mya for X_1X_2Y and ~1 Mya for XY_1Y_2, which accelerate speciation rates in the genus. The evolution of sex chromosomes in *Harttia* is followed not only by structural rearrangements but also by the putative recruitment of genes associated with reproductive and physiological functions, as indicated by gene ontology analysis. Together, these findings underscore the potential contribution of multiple sex chromosome systems and their turnovers in accelerating speciation rates in teleosts.

Keywords: SNP, phylogenetics, DArT-seq, sex-linked markers, probabilistic modeling

1. Introduction

In the canonical model of sex chromosome evolution, the emergence of a sex-determining gene is followed by the suppression of recombination around this locus, allowing the accumulation of sexually antagonistic alleles and other sex-linked sequences (Muller, 1918; Ohno, 1966). Structural rearrangements of chromosomes, such as inversions, might further consolidate this recombination suppression, resulting in the gradual differentiation and heteromorphy of the sex chromosomes (Graves, 2006). Nonetheless, before these chromosome rearrangements in regions where recombination persists, such as the pseudoautosomal region (PAR), sex-linked loci may still recombine between the X and Y or Z and W chromosomes (Zhu et al., 2025). These dynamics are particularly relevant in species exhibiting homomorphic sex chromosomes, where recombination suppression may be either partial or recent (reviewed in Charlesworth, 2017). Comprehending the inheritance patterns, chromosomal locations, and evolutionary trajectories of sex-linked markers is crucial for elucidating the origins and diversity of sex-determination systems (Kratochvíl et al., 2021; Zhu et al., 2025).

Multiple sex chromosome systems originate from chromosomal rearrangements that occur in simple systems (XX/XY or ZZ/ZW). These rearrangements may involve fissions of ancestral chromosome pairs or fusions with autosomes and are generally considered rare in eukaryotes (White, 1940; Kitano and Peichel, 2012; Pokorná et al., 2014; Pennell et al., 2015), found in only about 100 fish species (reviewed in Sember et al., 2021; Wang et al., 2022). However, our understanding of the evolution of sex chromosomes remains largely shaped by studies conducted in a limited number of model organisms, which typically possess heteromorphic sex

chromosomes at advanced evolutionary stages, thus providing a restricted view of the diversity and complexity of sex determination systems found in nature (Zhu et al., 2025).

In this context, the Neotropical armored catfish *Harttia* (Siluriformes: Loricariidae) is emerging as an exceptional model system to study multiple sex chromosomes with distinct degrees of degeneration. Comprising 28 valid species (Fricke et al., 2025), this monophyletic genus (Rapp Py-Daniel, 1997; Covain et al., 2016; Londoño-Burbano and Reis, 2021) is distributed across rheophilic habitats of the Brazilian and Guiana Shields. *Harttia* exhibits the highest number of multiple sex chromosome systems among fish, with about 28% of species displaying heteromorphic sex chromosomes (Sassi et al., 2024), a proportion matched only by *Notobranchius* killifishes (Krysanov and Demidova, 2018; Štundlová et al., 2022; Hospodářská et al., 2025). These systems vary in complexity and differentiation, making *Harttia* a unique model for studying repeated sex chromosome turnover and independent origins of multiple sex chromosome systems. Conventional and molecular cytogenetic data revealed an exceptional diversity of 2n (from 52 to 62 chromosomes), and two independent male-heterogametic systems (**Figure 1**): the XX/XY_1Y_2 and its homologous XX/XY in species from South and Southeast Brazil, and the $X_1X_1X_2X_2/X_1X_2Y$ system with a corresponding XX/XY in Amazonian species (Centofante et al., 2006; Blanco et al., 2014; Sassi et al., 2020; Deon et al., 2020). The rare XX/XY_1Y_2 system, described for only nine fish species to date (reviewed in Deon et al., 2020), is found in three *Harttia* species: *H. carvalhoi* and *Harttia* sp. 1, originating from a sex chromosome-autosome translocation (SC-A) involving an ancestral XX/XY configuration (seen in *H. torrenticola*), with a subsequent reciprocal translocation with an additional autosomal pair giving rise to the XX/XY_1Y_2 seen in *H.*

intermontana (Centofante et al., 2006; Deon et al., 2020, 2022a,b). Conversely, in the Amazonian lineage, a fission of the ancestral XY system (likely the same seen in *H. rondoni*) is proposed to have led to the emergence of the X_1X_2Y system found in *H. duriventris*, *H. villasboas*, and *H. punctata* (Sassi et al., 2023a,b). Comparative analyses of satellite DNA content further reveal distinct degrees of differentiation among these systems, indicating multiple independent origins and divergent evolutionary trajectories (Deon et al., 2024; Sassi et al., 2025).

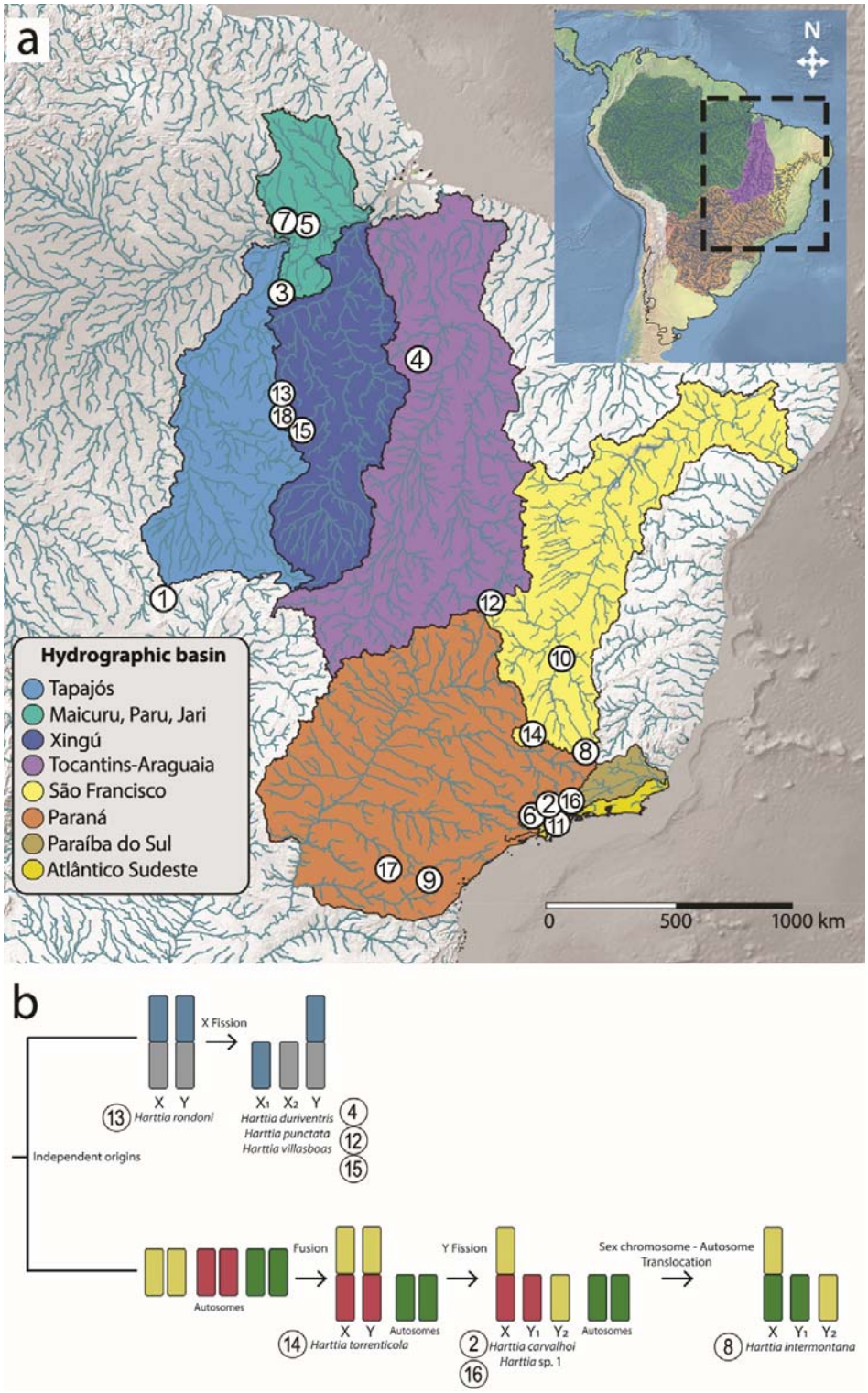

Figure 1. a) Partial Brazilian map indicating sample sites (circles) and river basins (colored areas). Numbering follows Supplementary Table 1. **b)** Schematic view of the proposed evolutionary pathways of *Harttia* sex chromosomes, based on previous cytogenetic data from Centofante et al. (2006), Blanco et al. (2014), Deon et al. (2020, 2022a, b, 2024), and Sassi et al. (2020, 2021, 2023a, b, 2025).

Without the availability of a reference genome, complexity reduction techniques have proven to be powerful tools for genomic research in non-model organisms (e.g., Nedoluzhko et al., 2021; Kirschner et al., 2022; Suchan et al., 2024; Knief et al., 2024). These approaches offer a cost-effective means of generating thousands of molecular markers, suitable for investigating genetic polymorphisms, assessing population structure, and exploring patterns of genome evolution (Davey et al., 2011). Analyses using large nuclear marker datasets provide higher resolution and assist in overcoming issues such as incomplete lineage sorting and restricted taxon sampling (Mirarab et al., 2016; Simmons & Gatesy, 2021). DArTseq (Diversity Arrays Technology sequencing) (Jaccoud et al., 2001) has emerged as a widely used method due to its ability to target low-copy and predominantly active genomic regions, which may include sex-specific loci, before high-throughput sequencing (Wenzl et al., 2004). These features have enabled DArTseq applications in a broad range of taxa and research areas, including genetic diversity, hybridization, admixture, phylogeography, phylogenetics, and the identification of sex-linked markers (Lambert et al., 2016; Baloch et al., 2017; Melville et al., 2017; Alam et al., 2018; Sopniewski et al., 2019; Aznar-Fernández et al., 2020; Mujyambere et al., 2024). Sex-linked markers provide key insights into the localization and structure of sex-determining regions, offering a molecular entry point into the evolutionary processes that shape sex chromosome systems (Lambert et al., 2016).

In this current study, we performed DArTseq in 17 *Harttia* species and one outgroup species (*Farlowella* sp.) to examine the genomic architecture of sex chromosome evolution in this dynamic genus (**Table 1**). Our primary objective was to identify the likely mechanisms underlying the diversity of multiple sex chromosomes in the genus. To this end, we focused on identifying putative sex-linked markers and

analyzing their distribution across species with different sex chromosome systems while also investigating their putative functions. We established a comprehensive phylogenetic tree utilizing SNP data, incorporating spatial and cytogenetic information by reconstructing ancestral distribution areas and analyzing chromosome number evolution through probabilistic modeling. Our data suggests that a rapid turnover of multiple sex chromosomes, from an ancestral XY, likely influences the diversification rates of *Harttia*.

2. Results

2.1 Evolutionary relationships in Harttia

A total of 95,305 SNPs and 282,275 SilicoDArT (presence and absence) loci were generated for 107 individuals from 17 *Harttia* and one *Farlowella* species. The resulting phylogeny, constructed using 1,381 SNP loci after stringent filtering, grouped all *Harttia* species into three primary clades, each exhibiting strong geographic coherence (**Figure 2a**). Exceptionally, *Harttia* sp. 2 was placed as a single ancestral branch to all remaining *Harttia*, not included in any of the three clades. Clade I comprises species from the Guiana Shield drainages (*H. fowleri* and *H. guianensis*). At the same time, Clade II included species from Amazon Brazilian Shield drainages, specifically the Xingu, Tapajós, and Tocantins-Araguaia River Basins (*H. duriventris*, *H. dissidens*, *H. punctata*, *H. rondoni*, *H. villasboas*, and *Harttia* sp. 3); and Clade III contained species distributed across Southeastern and South Atlantic drainages and from the La Plata basin (*H. carvalhoi*, *H. torrenticola*, *H. intermontana*, *H. longipinna*, *H. gracilis*, *H. loricariformis*, *H. kronei*, and *Harttia* sp. 1) (**Figure 2a**). The divergence between *Harttia* and *Farlowella* was estimated at ~30 million years ago (Mya), with Clade I split about 10 Mya and the divergence between

Clades II and III taking place at ~6 Mya. The origin of multiple sex chromosome systems was inferred at 5.7 Mya for Clade II (X_1X_2Y system) and at 1.3 Mya for Clade III (XY_1Y_2 system). The Principal Component Analysis (PCA) of autosomal SNPs (PC1 = 28.5%, PC2 = 18.9%) identified five distinct clusters aligned with phylogenetic clades and geographic distributions **(Supplementary Figure 2)**, categorizing *Harttia* species into three primary clusters, while *Harttia* sp. 2 and the outgroup *Farlowella* sp. constituted separate groups. The complete phylogeny with all individuals is presented in **Supplementary Figure 1**, and complete mean time-calibration estimates are provided in **Supplementary Table 2**.

When examining the number of lineages over time, two major shifts can be identified (**Figure 2b, arrows**). These shifts overlap with splitting times that are mostly related to species with multiple sex chromosomes (**Figure 1a**). Indeed, State-dependent diversification analyses with the Binary State Speciation and Extinction model (BiSSE) revealed substantial differences in speciation rates associated with the presence or absence of multiple sex chromosomes. Lineages with simple sex chromosome systems (state 0) exhibited a markedly lower speciation rate (λ_0 = 0.032, CI95% = 0.026-0.290) than multiple sex chromosomes (state 1; λ_1 = 0.941, CI95% = 0.485-3.064). The turnover rate for (ε = 1.040, CI95% = 0.776-1.230), calculated as the ratio between extinction and speciation suggests that extinction is approximately equal to speciation in this group. Additionally, the estimated transition rate from the absence to the presence of multiple sex chromosomes ($q_{0\leftrightarrow1}$) indicates a moderate probability of trait evolution over time (0.375, CI95% = 0.202-1.530). These modeling results suggest a strong association between the presence of multiple sex chromosomes and increased diversification rates in *Harttia* (p-value =

0.005), with lineages carrying these systems exhibiting substantially higher speciation rates compared to those without (**Figure 2c, Table 2**).

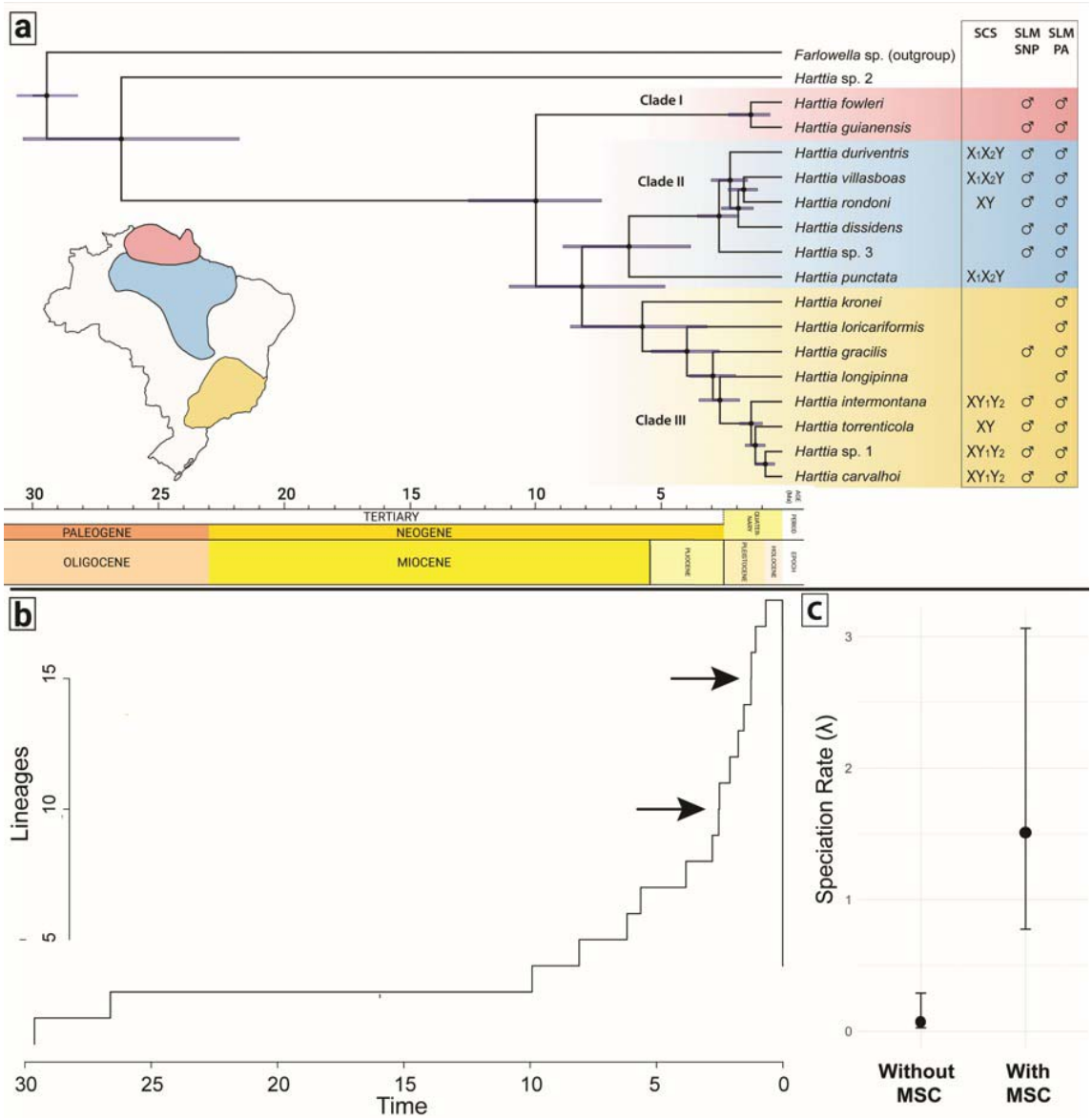

Figure 2. **Evolutionary relationships in *Harttia*. a)** Time-calibrated maximum likelihood phylogenetic relationships of *Harttia* species, using *Farlowella* sp. as an outgroup, recovered from 1,381 autosomal SNPs generated by DArTSeq from 108 individuals. Clade colors correspond to their distribution indicated in the map. Cytogenetically described sex chromosome systems are indicated (SCS). Sex-linked markers, either SNPs or SilicoDArT (PA), are presented using the male symbol to indicate male heterogamety (XY). Node bars correspond to the 95% HPD interval of

divergence times. **b)** Lineage through time plot, with arrows indicating major shifts in the number of lineages and corresponding to fusion events demonstrated above. **c)** Speciation rates in clades with and without multiple sex chromosomes inferred by BiSSE.

Table 2. Parameter estimates from the BiSSE model evaluating the association between the presence of multiple sex chromosomes and diversification rates. Speciation rates (λ) are reported separately for lineages without (state 0) and with (state 1) multiple sex chromosomes. Turnover rate (ε) corresponds to the extinction/speciation ratio. The transition rate ($q_{0\leftrightarrow1}$) reflects the rate of changes between the two states. Estimates are presented alongside their 95% confidence intervals.

Parameter	Estimate	95% CI
Speciation in clades without multiple sex chromosomes (λ_0)	0.032	0.026 - 0.290
Speciation in clades with multiple sex chromosomes (λ_1)	0.941	0.485 - 3.064
Turnover (ε)	1.040	0.776 - 1.230
Transition rate ($q_{0\leftrightarrow1}$)	0.248	0.202 - 1.530

2.2 Sex-linked markers

The likelihood of randomly identifying a sex-linked marker was determined to be 5.87×10^{-8}, suggesting that just 0.005 of the 95,305 SNPs would be expected to display random sex linkage, so confirming that the sampling effort was enough to identify reliable sex-linked markers across the species. Across all samples, we identified 443 sex-linked markers: 95 XY and 16 ZW markers from the SNPs dataset and 316 XY and 16 ZW markers from the SilicoDArT dataset (**Figure 3; Supplementary Data 1 and 2**). PCA of the sex-linked SNPs (**Supplementary**

Figure 2) revealed three main clusters: one composed solely of *H. intermontana*, a second grouping *H. carvalhoi*, *Harttia* sp. 1, and *H. torrenticola*, and a third containing the remaining species, with a minor subcluster of *H. gracilis*. Using a 100% similarity threshold, we identified three shared sex-linked SNPs and 33 shared SilicoDArT markers (**Supplementary Table 3**). Shared sex-linked markers were detected between two groups: i) *H. carvalhoi* and *H. intermontana* (XY_1Y_2 system) and ii) a subset of species within Clade II, all in both groups corresponding to XY SLM.

Gene ontology analysis revealed sex-linked markers associated with distinct biological processes and molecular functions (**Figure 3b**). For SNP data, GO terms related to biological processes of sensory systems (visual and auditory), gamma-aminobutyric acid (GABA) biosynthesis and shunt, and positive regulation of actin filament and filopodium were identified. For SilicoDArT, processes related to cyclic guanosine monophosphate (cGMP) were identified, as well as processes of transcription regulation, cell adhesion, and response to oxygen levels. Detailed proportions and molecular functions are presented in **Figure 3b**. Two of the shared SilicoDArT between *H. carvalhoi* and *H. intermontana* were recovered in B2GO analysis, one corresponding to the GO Term cyclic nucleotide-gated channel beta-1 isoform X1 (Biological process: cGMP-mediated signaling) and the second to dihydropyrimidine dehydrogenase [NADP(+)] (Biological process: response to O_2 levels).

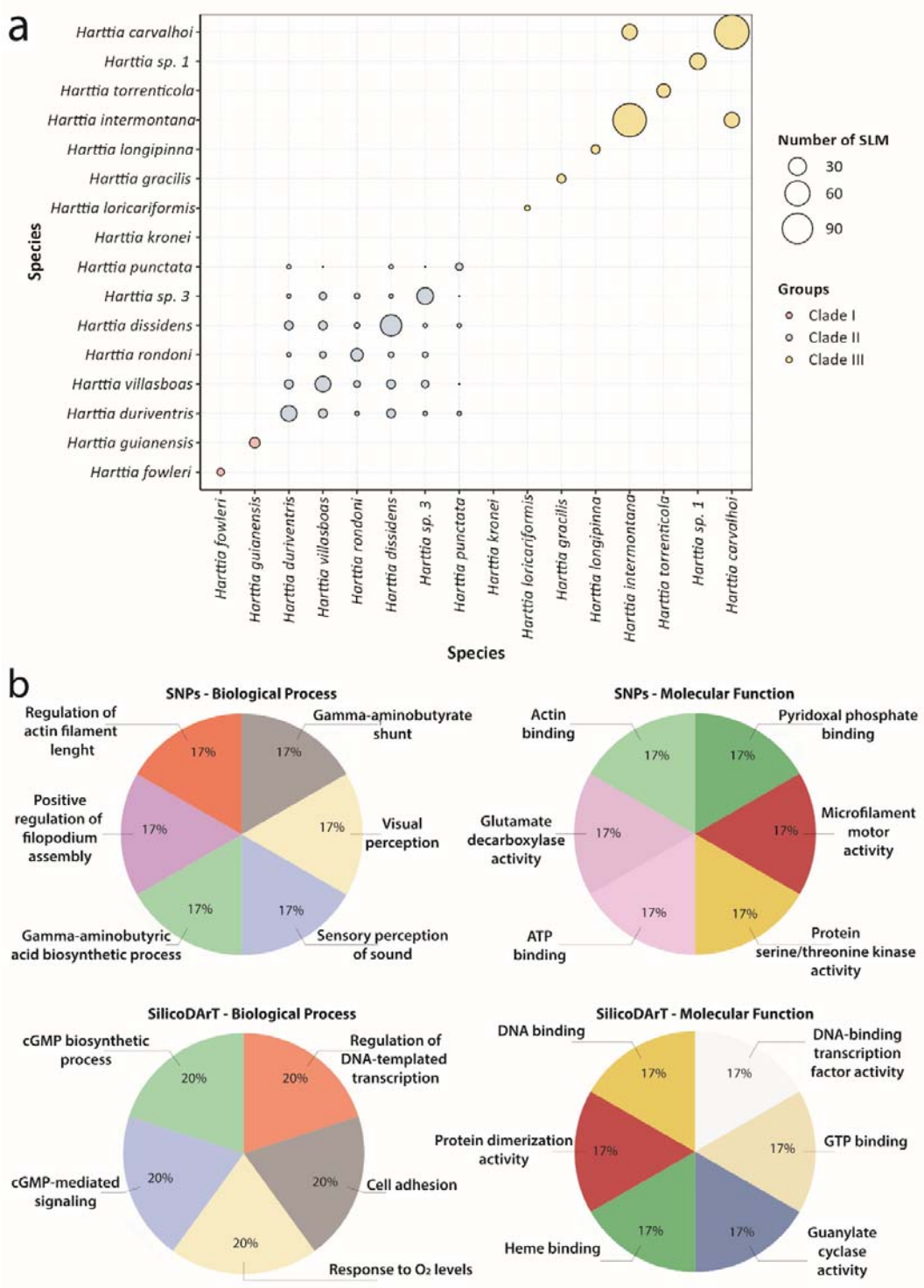

Figure 3. **Summary of sex-linked markers in *Harttia*. a)** Bubble plot showing the number of sex-linked markers per species, colored according to the clade they belong as shown in Figure 2. **b)** Pie charts indicating the biological processes (left) and the molecular function (right) GO terms recovered from Blast2GO among the SNP (first line) or Silico DArT (second line) data.

2.3 Biogeographical modeling and ancestral karyotype

The DIVALIKE model was selected as the best-fitting model based on AICc scores (**Table 3, Figure 4a**). Although likelihood scores between DEC and DIVALIKE models showed minimal variation, the estimated ancestral ranges diverged notably after the 23 Ma time slice (see **Supplementary Figure 3** for DEC estimates). ΔAIC values indicated only a marginal improvement for DIVALIKE over DEC, the same occurring for Akaike weights (W_i), indicating a little uncertainty between them. Both models converged on similar ancestral area reconstructions after the 10 Ma threshold. The most inclusive *Harttia* clade (excluding *Harttia* sp. 2) was inferred to have occupied either the Eastern Amazon or the Southern and Southeastern Atlantic drainages. The most recent common ancestor of Clade III was likely restricted to the Atlantic South and Southeastern drainages, whereas Clade II appears to have been confined to the Amazonian Brazilian Shield. DIVALike suggested an ancestral distribution along the Atlantic coastal drainages for the whole *Harttia* clade, with the ancestor of *Harttia* and *Farlowella* likely ranging either on the Atlantic South and Southeastern drainages or the Amazonian Brazilian Shield.

Table 3. Models implemented in BioGeoBEARS with their respective Log-likelihood (lnL), dispersal (d), and extinction (e) parameters, corrected Akaike information criterion (AICc), difference in AICc values compared to the best-fit model (ΔAIC), and Akaike weights (W_i).

Model	lnL	*d*	*e*	AICc	ΔAIC	Weight (W_i)
DEC	-39.28528	0.0268696	0.0304716	82.59056	0.97624	0.38
DIVALike	-38.80716	0.02924266	0.02305116	81.61432	0	0.62
BayAreaLike	-45.32449	0.03725671	0.08521665	94.64898	13.03466	0.0009

The ancestral 2n found at the root of the phylogeny proposed by the model Dys was 2n = 62, indicating that events of descending dysploidy (chromosome fusions) were predominant throughout *Harttia* chromosomal evolution. For the *Harttia*

clade (excluding *Farlowella*), the same ancestral 2n was found. The same ancestral 2n was identified for the *Harttia* clade, excluding *Farlowella*. In clade III, the ancestral diploid number for species exhibiting cytogenetically identifiable sex chromosomes (*H*. *intermontana*, *H*. *torrenticola*, *H*. *carvalhoi*, and *Harttia* sp. 1) is 2n = 56, while in clade II (most comprehensive clade including *H. punctata*, *H. duriventris,* and *H. villasboas*), it is 2n = 58 (**Figure 4b, Supplementary Data 3**).

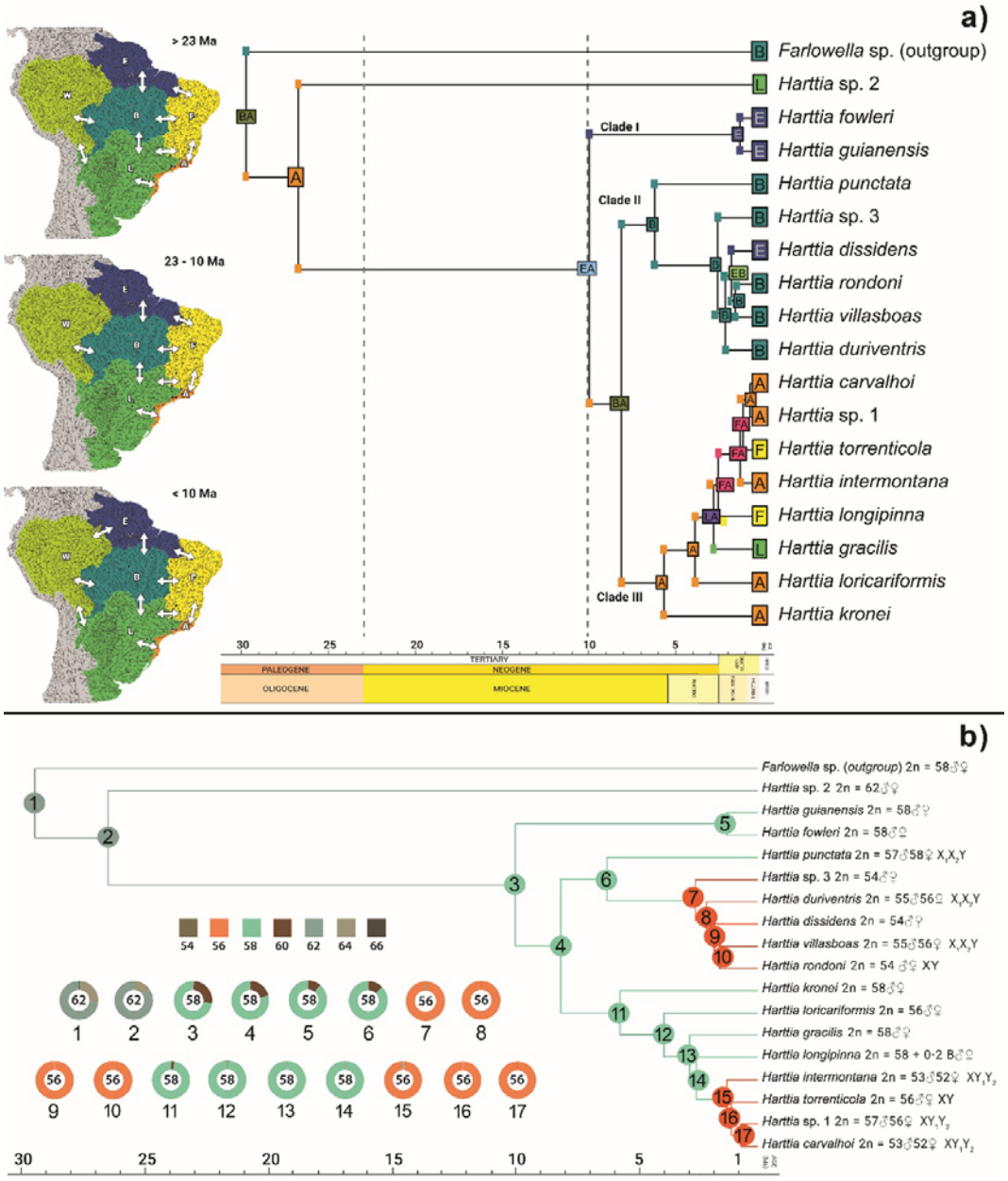

Figure 4. Biogeographic and karyotype modeling for the ancestral characters of *Harttia*. a) Ancestral range of *Harttia* estimated from the best model DIVALike in BioGeoBEARS. Dashed lines correspond to the three time slices defined for modeling: > 23 Ma, 23-10 Ma, and < 10 Ma, which are also represented in the maps with the connections allowed at each (white arrows). The color of tips in phylogeny corresponds to the same color in the map. **b)** The evolution of diploid numbers in *Harttia* was inferred in ChromEvol v2.0 with the Dys model. Each branch is colored with the same color indicated in the legend for its respective ancestral 2n. Pie charts indicate the probability of the ancestral 2n recovered for each node, indicated by numbers (1-17) in the nodes of the phylogenetic tree. The diploid number and sex chromosome system of the species are shown after their names.

3. Discussion

Our study demonstrates that the diversification of *Harttia* is driven by a combination of biogeographical events, karyotype restructuring, and multiple independent origins of sex chromosome systems. We demonstrate that *Harttia* diversification occurred primarily over the past 10 million years, coinciding with major geological and hydrological changes in South America. Notably, the emergence of multiple sex chromosome systems occurred during ~5.6 and ~1.2 Mya and appears to have accelerated speciation rates, highlighting their important role in the evolution and speciation of the genus. These findings reshape our understanding of the genus and present *Harttia* as a model for studying rapid and recurrent sex chromosome turnover and its role in speciation.

The nuclear-based phylogeny based on 1,381 markers resolves three major *Harttia* clades but differs from previous mitochondrial and morphological studies. While broadly consistent with earlier studies (Covain et al., 2016; Londoño-Burbano & Reis, 2021), our topology reveals key discrepancies such as the placement of *H. fowleri* within clade I instead of clade II, and a distinct sister-group relationship involving *H. dissidens*, indicating more complex interspecific relationships than previously recognized. In our phylogeny, *H. dissidens* is sister to the *H. rondoni* + *H. villasboas* clade, with this group forming a sister lineage to the *H. duriventris*, and all these species sister to *H. punctata*, the earliest diverging species in clade II at ~6 mya. In contrast, Londoño-Burbano and Reis (2021) recovered *H. dissidens* as more ancestral to the whole clade II, while in Covain et al. (2016), *H. dissidens* was placed as a sister to most species, with only *H. punctata* showing an older diversification. Notably, *Harttia* sp. 2 was recovered herein as deeply divergent from the remaining *Harttia* species, with an estimated split occurring ~25 Mya. This lineage exhibits a

distinct karyotype, which is highly similar to that reported in *H. absaberi* (Rodrigues, 2010), with 2n = 62 chromosomes and a high number of interstitial telomeric sites (ITS) (Deon et al., 2020). SLMs are found in all *Harttia* species but *Harttia* sp. 2, supporting a distinction of the latter from the remaining *Harttia* species (**Figure 3**). Indeed, *H. absaberi* was included in the molecular and morphological phylogeny presented by Cherobim (2021), who recovered it as more closely related to other Loricariinae genera than to *Harttia*, suggesting it may warrant placement in a separate genus. Although our sampling included only a single outgroup (*Farlowella*), which diverged from *Harttia* ~30 Mya, the combined evidence from phylogenetic distance, divergence time, and cytogenetic data therefore supports the hypothesis that *Harttia* sp. 2, like *H. absaberi*, may not belong to *Harttia* sensu stricto.

Biogeographically, *Harttia* diversification mirrors Neotropical River evolution (**Figure 4a**). The divergence of major clades aligns with the Miocene uplift of the Andes Mountain range that led to the reconfiguration of most drainage systems in South America, especially in the Amazonian region. The distribution of clade II species across formerly interconnected basins (e.g., Tocantins-Araguaia, Xingu, Tapajós) reflects historical dispersal followed by vicariant speciation, a pattern corroborated by similar trends in other loricariid taxa and the highly similar ichthyofauna of those basins, as reported previously in other lineages such as *Cynolebias* spp., *Centromochlus schultzi*, and several Prochilodontidae (Hubert and Reno, 2006; Rossetti et al., 2007; Lima and Ribeiro, 2011; Albert et al., 2018; Roxo et al., 2019; Dagosta et al., 2020). Indeed, the redirection of river courses occurred in the late Miocene, especially proto-Tapajós, proto-Xingu, and proto-Tocantins-Araguaia (Albert et al., 2018), the development of mega-wetlands, and the formation of interfluves such as the Purus Arch and the Serra do Cachimbo introduced new

opportunities for both dispersal and vicariant isolation among freshwater organisms, particularly loricariids (Cassemiro et al., 2023), which agrees with the patterns here observed for *Harttia*. Notably, patterns of biogeographical diversification seen in clade III coincide with the time when the uplift of the Serra do Mar and Serra da Mantiqueira Mountain ranges occurred. These events have isolated certain portions of the La Plata Basin from the Atlantic South and Southeastern Drainages, so as from the São Francisco River Basin (Cassemiro et al., 2023, 2025), leading to vicariant processes among their similar ichthyofauna, as also observed for *Salminus* spp. (Machado et al., 2018).

Our modeling approaches on both chromosome evolution (ChromEvol) and biogeographical patterns (BioGeoBEARS) support the ancestors of *Harttia* with a distribution in either the Eastern Amazon or Southeast/South Atlantic drainages. The ancestral karyotype was possibly composed of 2n = 58 chromosomes and an XY sex chromosome system, likely in early stages of differentiation (**Figure 5**). Findings thus corroborate earlier hypotheses based on comparative cytogenetics that proposed the same 2n as the ancestral state (Blanco et al., 2017; Deon et al., 2020), therefore, confirming the independent reductions of karyotypes from 2n = 58 to 2n = 56 in *H. loricariformis*, *H. villasboas*, and *H. duriventris*, and subsequent reductions of 2n = 54 in *H. rondoni* and *Harttia* sp. 3 (Deon et al., 2022a; Sassi et al., 2023a). These karyotype reductions were mostly facilitated by centric fusions, as indicated by our ChromEvol inference (**Figure 4b**). Nevertheless, these chromosome rearrangements did not involve chromosomal components associated with the intricate multiple sex chromosome systems outlined in the genus (Deon et al., 2022b; Sassi et al., 2023a). The dissociation of autosomal and sex chromosomes dynamics underscores the intricate interaction of lineage-specific and conserved processes, such as

Robertsonian translocations and inversions that influence chromosome evolution in this group. Notably, breakpoints in *Harttia* are probably linked to the instability of rDNA loci (Deon et al., 2020, 2022a, b; Sassi et al., 2020, 2023a, b), particularly the 18S rDNA, which is not involved in the creation of the XY_1Y_2. Ribosomal sequences are known to compose evolutionary breakpoint regions among loricariids (e.g., Barros et al., 2017; Glugoski et al., 2018), since they increase genomic instability given the facilitated formation of double-strand breaks by the high transcriptional activity (Berthelot et al., 2015; Warmerdam et al., 2019).

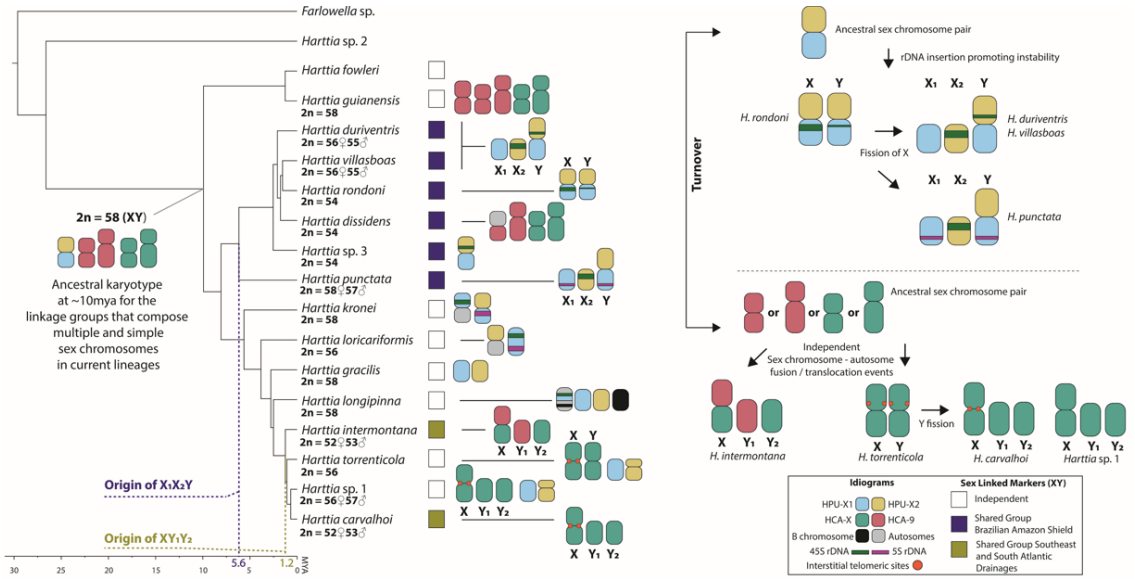

Figure 5. Rapid turnover of multiple sex chromosomes in *Harttia*. A compilation of previous cytogenetic data (Centofante et al., 2006; Blanco et al., 2014, 2017; Deon et al., 2020, 2022a, b, 2024; Sassi et al., 2020, 2021, 2023a, b, 2025) and the results herein obtained with the main hypothesis for the sex chromosome evolution in *Harttia*. Chromosome colors follow the homology patterns established by Deon et al. (2022a, b) and Sassi et al. (2023a, b). Idiograms are presented for each species-specific chromosome, while those pairs not shown in each species tip indicate the conservation of the ancestral state, as depicted on the left. Chromosomes are not drawn to scale.

Our study demonstrated that recurrent turnover and independent evolution of multiple sex chromosomes are key mechanisms in the evolution of *Harttia*, reflecting the dynamic nature of sex chromosomes in this group. Across diverse lineages, including plants, fish, and reptiles, recurrent turnover of sex chromosomes within a relatively short evolutionary timescale has been reported (e.g., Keating et al., 2021; Kabir et al., 2022; Wang et al., 2022; Yi et al., 2024; Hayashi et al., 2024; Wang et al., 2024; Zheng et al., 2025), however, none is comparable with *Harttia*, where these events occur within a very short timeframe (~4 My). The arising of multiple sex chromosome systems usually results in postzygotic isolation, mainly due to segregation incompatibilities (White, 1940; Furman et al., 2020; Sember et al., 2021). Rearrangements are also responsible for recombination suppression, which reduces gene flow near rearranged regions (Yannic et al. 2009; McGaugh and Noor 2012; Toups et al. 2019). Furthermore, genes that contribute to reproductive isolation can accumulate on the neo-sex chromosomes, contributing to the speciation process (Kitano et al., 2009; Kitano and Peichel, 2012). We hypothesize that a similar process may have happened on both rearrangement events, which resulted in XY_1Y_2 and X_1X_2Y systems, leading to faster reproductive isolation and speciation. This process was similarly documented in sticklebacks (Kitano et al., 2009; Kitano and Peichel, 2012) and was also proposed for other species such as *Brenthis* butterflies (Mackintosh et al., 2023), African cichlids (Lande et al., 2001; El Taher et al., 2021), and rock wallabies (Potter et al., 2017). Among vertebrates, several mechanisms can drive sex chromosome turnover, including the acquisition of novel sex-determining mutations, translocations of pre-existing sex-determining (SD) genes, chromosomal fusions, and, in some cases, hybridization between populations with distinct SD systems (Kitano and Peichel, 2012; Yoshida and Kitano, 2012; Faber-Hammond et

al., 2015; Graves, 2016; Palmer et al., 2019; Bracewell and Bachtrog, 2020; Sember et al., 2021; Bertho et al., 2021; Kabir et al., 2022). Given the absence of sympatric populations of *Harttia*, turnover driven by hybridization events appears unlikely. Instead, the emergence of the XY_1Y_2 system may be best explained by Y-autosome translocation, a mechanism widely reported in teleosts with multiple sex chromosome systems (Sember et al., 2021). In contrast, the X_1X_2Y systems observed in clade II are more consistent with turnovers mediated either by novel SD mutations or translocations of ancestral SD genes. Notably, the association of ribosomal DNA (rDNA) sites with sex chromosomes in species of clade II suggests that rDNA insertions could act as catalysts for recombination suppression by breaking the linkage groups of SD.

Theoretical models suggest that when autosomes harbor genes with sexually antagonistic effects—beneficial to one sex but detrimental to the other—selection may favor the evolution of new sex-determining loci, the transposition of existing ones, or chromosomal fusions that link these genes to sex chromosomes (Charlesworth and Charlesworth 1980; van Doorn and Kirkpatrick 2007). Such processes have been implicated in other fish lineages like Lake Malawi cichlids, where a female-determining locus became linked to a gene involved in sexually dimorphic pigmentation (Roberts et al. 2009). Our gene ontology analysis of SLM suggests that the evolution of sex chromosomes in *Harttia* may be accompanied by the recruitment of genes with diverse physiological roles, such as those from sensory systems, a scenario also observed for Varanidae lizards (Dobry et al., 2023; Zhu et al., 2025), cichlids and poecilids fishes (Kottler and Schartl, 2018). Pathways linked to gamma-aminobutyric acid (GABA) biosynthesis and signaling are also found among *Harttia*'s SLM. GABA plays a pivotal role in vertebrate reproduction, including

in teleosts, where it stimulates the release of luteinizing hormone during critical stages of gonadal development (Trudeau, 2022; Gabilondo et al., 2021). Interestingly, cGMP-mediated signaling has also been recovered among the GO terms of SLM in *Harttia*, with this implicated in oocyte maturation in zebrafish *Danio rerio* (Li et al., 2018), which may indicate a role of sexually antagonistic loci in the evolution of multiple sex chromosomes of *Harttia*.

In conclusion, our study presents the first genome-wide phylogenetic framework for the armored catfish genus *Harttia*, offering new insights into its evolutionary history, chromosomal evolution, and sex chromosome dynamics in teleosts. While broadly congruent with previous hypotheses, our phylogeny reveals several key topological differences, likely attributable to the increased resolution afforded by genome-wide data. Divergence time estimates highlight a relatively recent radiation of *Harttia* sensu stricto over the past 10 million years, tightly associated with major geological and hydrological transformations in South America driven by the formation of the Amazon River and the rise of the mountain ranges, and accelerated by the turnover of multiple sex chromosomes at 5.6 and 1.2 mya. Our results further support the hypothesis that *Harttia* sp. 2, like *H. absaberi*, falls outside *Harttia* sensu stricto, reflecting deep phylogenetic divergence corroborated by both cytogenetic and molecular evidence, and challenging the monophyly of the genus. Chromosome evolution in *Harttia* is characterized by a dynamic interplay of variation in diploid numbers, lineage-specific reductions via centric fusions, and recurrent turnovers of sex chromosomes, leading to the independent origins of complex multiple sex chromosome systems, which seem crucial in establishing the diversity of the genus. Notably, the integration of sex-linked marker analysis suggests that the evolution of sex chromosomes in *Harttia* is followed not only by structural

rearrangements but also by the recruitment of genes associated with reproductive and physiological functions. Together, these findings underscore the potential contribution of multiple sex chromosome systems and their turnovers in accelerating speciation rates when compared to the simple chromosome system representatives. It also reveals the intricate evolutionary processes shaping both genome structure and diversification in Neotropical fishes. Future studies incorporating broader taxonomic and genomic sampling will be essential to further refine the evolutionary history of *Harttia*, a remarkable repository of multiple sex chromosome systems.

4. Materials and Methods

4.1 Sampling

We selected all *Harttia* species with available cytogenetic data, following those described in **Table 1**. The sex of the individuals was recovered from the morphological investigation of the gonads. Fish were anesthetized and euthanized with Eugenol, as approved by the Ethics Committee on Animal Experimentation of the Universidade Federal de São Carlos (Process number CEUA 7994170423).

4.2 DArTseq and sex-linked markers

Liver tissue samples were collected from six individuals of each species (three males and three females), comprising a full dataset of 107 individuals, and submitted to Diversity Arrays Technology (DArT) Pty Ltd (University of Canberra, Canberra, Australia) for genotyping by sequencing. Briefly, DNA samples were digested with the restriction enzymes *PstI* and *SphI*, followed by adapter ligation and 30 cycles of PCR amplification. Amplified products were sequenced using single end reads on an Illumina HiSeq2000 platform. Data filtering and quality control were performed by

DArT Pty Ltd, excluding loci with reproducibility <90% and read depths <3.5× for SNPs and <5× for Silico-DArT markers. For the characterization of sex-linked markers, both SNPs and Silico-DArT loci with missing data were not included in the analysis. For all remaining analyses (PCA, phylogenetic inference), loci with high frequencies of null alleles (call rate <0.85) were filtered out.

Candidate sex-linked markers were identified following the pipeline proposed by Lambert et al. (2016). DArTseq datasets were first organized per species and sex, grouping males and females separately. For each individual, SNPs were tallied by heterozygous genotypes (coded as "2") for each sex, using counts of homozygous genotypes (either "0" for the reference or "1" for the alternate allele) as the baseline. Given that, sex-linked SNPs were defined as SNPs with all individuals from one sex presenting heterozygous genotypes and all individuals from the other sex with homozygous genotypes. On the other hand, sex linked markers from Silico-DArT data (presence and absence) corresponded to those with the presence of the restriction recognition sites in all individuals from one sex but not the other. The expected rate of random sex linkage was calculated using the formula proposed by Lambert et al. (2016), based on sample size and the number of high-quality SNPs generated per sequencing plate. Given the potential bias introduced by complexity reduction methods, random sex linkage was estimated at the genus or sequencing plate level.

Sequences of the sex-linked SNPs and SilicoDArT loci were then compiled into a secondary dataset and converted into FASTA format. Functional annotation of candidate markers was performed with Blast2GO (Conesa et al. 2005) using the NCBI Actinopterygii database (taxon ID: 7898) and default parameters. To assess potential homology among sex-linked markers, multiple sequence alignments were

performed in Geneious (Geneious Prime v2025.1, Dotmatics, Boston, USA) using the MUSCLE algorithm with default settings. Pairs of sequences exhibiting 100% similarity were identified from the pairwise distance matrix using a custom R script.

4.3 Time-calibrated phylogeny and Principal Component Analysis

We inferred the evolutionary history of *Harttia* species by Maximum Likelihood using RAxML-ng (Stamatakis, 2014). After filtering out SNPs under selection (5 sequences) using Bayescan (Foll and Gaggiotti, 2008), a total of 1,381 SNPs of 107 individuals from 18 species (17 *Harttia* + 1 *Farlowella*) were included in the analysis. First, model selection was conducted in ModelTest-NG with seed number defined as “12345”, and all models supported by RAxML-ng were tested (Darriba et al., 2020). ModelTest-NG indicated HKY+I+G4 as the model with the smallest AIC (lnl -118802.5778) and HKY+I as the model with the lowest BIC (lnl 240039.7218). The analysis was conducted with 50 initial maximum parsimony trees and 50 initial random trees. The analysis was performed with a total of 1000 bootstraps and mapped into the best tree. The tree with the highest log likelihood was used for time calibration. Finally, the tree was rooted using FigTree v.1.4.4 (Rambaut, 2018), defining *Farlowella* sp. as the outgroup.

Coalescent divergence times and population sizes were estimated under the Multispecies Coalescent Model using BPP (Yang, 2015) and calibrated to geological time with bppR (Angelis and dos Reis, 2015). BPP is comprehensive software for Bayesian Markov Chain Monte Carlo (MCMC) analysis, widely applied for species delimitation and divergence times estimation (Yang, 2015). We first performed an A00 method analysis (no species delimitation and fixed tree topology). To ensure the consistency of the estimations in our dataset (Flouri et al., 2018; Tiley et al., 2020;

Ortiz et al., 2021), we performed independent runs with random subsets of different sizes (300, 400, and 500 SNPs), each with triplicates starting at distinct seed numbers. We assumed a mutation rate (μ) of 3×10^{-9} based on the inferred rate of the *Malapterurus electricus*, the closest Siluriformes with μ data (Liu et al., 2024). We also adopted a divergence time estimation of 30 mya for *Harttia* and *Farlowella* based on the mean of estimates on TimeTree5 (Kumar et al., 2022). Considering these values, the theta prior was defined as an inverse gamma distribution of 3 0.002, and the tau prior was set as an inverse gamma distribution of 3 0.18. For this analysis, *Farlowella* was defined as the outgroup. Finetune was allowed, chain length was set to 400,000 generations, with a burn-in of 40,000, and sampling frequency was defined as 2. The first 15% of the samples of each run were discarded as burn-in, and each triplicate was concatenated. Effective sample size (ESS) values were checked on Tracer (Rambaut et al., 2018) to ensure that posterior distributions were adequately estimated. The final time calibrations were defined as the mean of the triplicate outputs with 95% HPD in bppR (**Supplementary Table 2**). We performed a time calibration using a prior node age, based on the mean divergence time of *Harttia* and *Farlowella* estimated on TimeTree5 (Kumar et al., 2022). To describe the temporal patterns of cladogenesis within the genus, we created a lineage-through-time plot (LTT plot) using ape 5.8 (Paradis and Schliep, 2019) on R (R Core Team, 2025).

Principal component analysis (PCA) was conducted using the R package dartR (Gruber et al., 2018; Mijangos et al., 2022). Two distinct datasets were defined, one containing all sex-linked SNPs and a second using the whole SNP dataset, excluding the sex-linked ones (here defined as autosomal SNPs). The most

representative PCs were selected for the plot, and the figure was constructed in Adobe Illustrator (Adobe Corporation).

4.4 Character state-dependent branching

We applied the Binary State Speciation and Extinction (BiSSE) model (Maddison et al., 2007) in R (4.3.1) with the package “hisse” (Beaulieu & O’Meara, 2016) to test whether the presence of multiple sex chromosomes is associated with differences in diversification rates. The binary dataset for the character “multiple sex chromosomes” was defined with two states: absence = 0 and presence = 1. We followed the strategy proposed in Lambert et al. (2023), to estimate state-specific speciation rates (λ_0 and λ_1), a single turnover rate ($\varepsilon = \mu/\lambda$) applied to both states, and a single transition rate ($q_{0\leftrightarrow 1}$) between trait states. Likelihood optimization employed an initial simulated annealing phase followed by refinement using a subplex routine to obtain maximum likelihood estimates for speciation rates (λ_0, λ_1), a common turnover rate (ε), and transition rate ($q_{0\leftrightarrow 1}$). Confidence intervals for parameter estimates were derived through likelihood profiling via the SupportRegionHiSSE function, sampling 1000 points within the likelihood support region. To assess whether differences in speciation rates between trait states were statistically significant, we performed a likelihood ratio test (LRT). This involved comparing a full model where speciation rates were allowed to vary between states ($\lambda_0 \neq \lambda_1$) to a constrained null model in which speciation rates were set equal across states ($\lambda_0 = \lambda_1$). The test statistics were calculated as twice the difference in log-likelihoods between the models, which was compared to a chi-squared distribution with one degree of freedom, revealing a p-value of 0.005559656.

4.5 Chromosome number evolution

Chromosome counts and a time-calibrated phylogenetic tree with branch lengths were analyzed in ChromEvol v2.0 (Glick and Mayrose, 2014) to infer ancestral chromosome numbers. We evaluated six default models incorporating ascending dysploidy (single chromosome gains) and descending dysploidy (single chromosome losses) under a time-homogeneous framework. Model adequacy was assessed based on the best-fitting model (Dys). The minimum chromosome number was set to n = 26, corresponding to the lowest value observed in both *Harttia carvalhoi* and *H. intermontana*. The maximum chromosome number was set to n = 31, based on the highest diploid count (2n = 62) recorded for *H. absaberi* and *Harttia* sp. 2, the latter included in our dataset.

4.6 Ancestral range estimation

The ancestral range of species was estimated using BioGeoBEARS (Matzke, 2018), implemented in R. Three models of range evolution were tested: the dispersal–extinction–cladogenesis (DEC) model (Ree and Smith, 2008), the likelihood version of DIVA - DIVALIKE (Ronquist, 1997), and BAYAREALIKE (Landis et al., 2013). Variants of these models incorporating a founder-event speciation parameter ("j") were not considered, as this parameter has been widely criticized (Ree and Sanmartín, 2018) and is unlikely to accurately represent dispersal in freshwater-restricted taxa where river connectivity is essential for gene flow.

Six freshwater ecoregions were defined based on the present-day distribution of species included in the analysis: Western Amazon (W), Eastern Amazon (E), Amazon Brazilian Shield (B), São Francisco and Northeastern drainages (F), Southern and Southeastern Atlantic drainages (A), and the La Plata basin (L).

Species distributions were compiled from original descriptions and related literature (Oyakawa et al. 2018) and cross-referenced with occurrence data obtained from GBIF, which were visualized in QGIS (**Supplementary Figure 4**). Given the high endemism of *Harttia* species, which typically do not span multiple regions, we set the maximum number of areas allowed per node to two. This strategy avoids over-constraining the model, as using only a single area per node is not recommended (Matzke, 2018).

To account for major historical changes in river connectivity, we defined three time slices based on Neotropical geological history, following frameworks established by Conde-Saldaña et al. (2025): >23 Ma, 23–10 Ma, and <10 Ma. These periods encompass key events in river capture and paleodrainage evolution of the Neotropical region (Albert et al., 2006, 2018, 2021; Tagliacollo et al., 2015; Montes et al., 2021). The map representing these connections was created using QGIS 3.28.2-Firenze using merged ecorregions from Abell et al. (2008).

Data availability statement

All the data and scripts used for this study are available at https://github.com/sassichico/harttia.

Acknowledgements

We appreciate the contributions of Osvaldo Oyakawa, Lúcia Rapp-Py Daniel for the identification of species used in this work, and to Claudio Oliveira, Vladimir Trifonov, José Maurício Barbanti Duarte, Francisco Langeani, and Orlando Moreira Filho for the valuable insights. We also thank Eliana Feldberg and all members of Laboratório

de Genética Animal - INPA, so as Marcelo Vicari, Luiz Henrique Silva, and Antonio Donizete, for the assistance in collecting specimens.

Study Funding

FMCS is currently funded by Conselho Nacional de Desenvolvimento Científico e Tecnológico (CNPq 200247/2025-5) and was supported during this study by FAPESP 2020/02681-9, 2022/04261-2, and 2023/08116-0. MBC was supported by FAPESP (2023/00955-2).

References

1. Abell R, Thieme ML, Revenga C, Bryer M, Kottelat M, Bogutskaya N, Coad B, Mandrak N, Balderas SC, Bussing W, et al. 2008. Freshwater Ecoregions of the World: A New Map of Biogeographic Units for Freshwater Biodiversity Conservation. *Bioscience* 58:403-414.
2. Alam SMI, Prasongmaneerut T, Gleeson D, Georges A, Sarre SD, Srikulnath K, Ezaz T. 2018. Sex-Determination mechanisms among populations within cryptic species complex of *Calotes* (Squamata: Agamidae: Draconinae). *DNA* 1:49-67.
3. Albert JS, Lovejoy NR, Crampton WGR. 2006. Miocene tectonism and the separation of cis- and trans-Andean river basins: Evidence from Neotropical fishes. *J South Am Earth Sci.* 21:14-27.
4. Albert JS, Val P, Hoorn C. 2018. The changing course of the Amazon River in the Neogene: center stage for Neotropical diversification. *Neotrop Ichthyol.* 16: e180033.

5. Albert JS, Bernt MJ, Fronk AH, Fontenelle JP, Kuznar SL, Lovejoy NR. 2021. Late Neogene megariver captures and the Great Amazonian biotic interchange. *Glob Planet Change*. 205:103554.
6. Angelis K, Dos Reis M. 2015. The impact of ancestral population size and incomplete lineage sorting on Bayesian estimation of species divergence times. *Curr Zool.* 61:874-885.
7. Aznar-Fernández T, Barilli E, Cobos MJ, Kilian A, Carling J, Rubiales D. 2020. Identification of quantitative trait loci (QTL) controlling resistance to pea weevil (*Bruchus pisorum*) in a high-density integrated DArTseq SNP-based genetic map of pea. *Sci Rep*. 10:33.
8. Baloch FS, Alsaleh A, Shahid MQ, Çiftçi V, Sáenz de Miera LE, Aasim M, Nadeem MA, Aktaş H, Özkan H, Hatipoğlu R. 2017. A whole genome DArTseq and SNP analysis for genetic diversity assessment in durum wheat from central fertile crescent. *PLoS One.* 12:e0167821.
9. Barros AV, Wolski MAV, Nogaroto V, Almeida MC, Moreira-Filho O, Vicari MR. 2017. Fragile sites, dysfunctional telomere and chromosome fusions: What is 5S rDNA role? *Gene*. 608:20-27.
10. Beaulieu JM, O'Meara BC. 2016. Detecting hidden diversification shifts in models of trait-dependent speciation and extinction. *Syst Biol*. 65:583-601.
11. Berthelot C, Muffato M, Abecassis J, Crollius HR. 2015. The 3D organization of chromatin explains evolutionary fragile genomic regions. *Cell Rep*. 10:1913-1924.
12. Bertho S, Herpin A, Schartl M, Guiguen Y. 2021. Lessons from an unusual vertebrate sex-determining gene. *Philos Trans R Soc Lond B Biol Sci*. 376:20200092.

13. Blanco DR, Vicari MR, Lui RL, Artoni RF, Almeida MC, Traldi JB, Margarido VP, Moreira-Filho O. 2014. Origin of the $X_1X_1X_2X_2/X_1X_2Y$ sex chromosome system of *Harttia punctata* (Siluriformes, Loricariidae) inferred from chromosome painting and FISH with ribosomal DNA markers. *Genetica.* 142:119–126.
14. Bracewell R, Bachtrog D. 2020. Complex evolutionary history of the Y chromosome in flies of the *Drosophila obscura* species group. *Genome Biol Evol*. 12:494-505.
15. Cassemiro FAS, Albert JS, Antonelli A, Menegotto A, Wüest RO, Cerezer F, Reis RE, Tan M, Tagliacollo V, et al. 2023. Landscape dynamics and diversification of the megadiverse South American freshwater fish fauna. *Proc Natl Acad Sci U S A*. 120:e2211974120.
16. Cassemiro FAS, Salgado AAR, Paixão RW, Rezende EA. 2025. The timing of large drainage rearrangement in South America: A study based on morphological and ecological evidence. *Geomorphology*. 468:109457.
17. Centofante L, Bertollo LAC, Moreira-Filho O. 2006. Cytogenetic characterization and description of an XX/XY_1Y_2 sex chromosome system in catfish Harttia carvalhoi (Siluriformes, Loricariidae). *Cytogenet Genome Res*. 112:320-024.
18. Charlesworth D. 2017. Evolution of recombination rates between sex chromosomes. *Philos Trans R Soc Lond B Biol Sci*. 372:20160456.
19. Charlesworth D, Charlesworth B. 1980. Sex differences in fitness and selection for centric fusions between sex-chromosomes and autosomes. *Genet Res*, 35:205-214.

20. Cherobim A, unpublished data, https://repositorio.unesp.br/entities/publication/32eef081-dd13-452f-949b-84968a795e84, last accessed August 08, 2025.
21. Conde-Saldaña CC, Melo BF, Roxo FF, Tagliacollo VA, Oliveira C, Albert JS. 2025. Landscape Evolution Drives Continental Diversification in Neotropical Freshwater Fishes of the Family Erythrinidae (Teleostei, Characiformes). *J Biogeogr*. 52:e15129.
22. Conesa A, Götz S, García-Gómez JM, Terol J, Talón M, Robles M. 2005. Blast2GO: a universal tool for annotation, visualization and analysis in functional genomics research. *Bioinformatics* 21:3674-3676.
23. Covain R, Fisch-Muller S, Oliveira C, Mol JH, Montoya-Burgos JI, Dray S. 2016. Molecular phylogeny of the highly diversified catfish subfamily Loricariinae (Siluriformes, Loricariidae) reveals incongruences with morphological classification. *Mol Phylogenet Evol*. 94:492-517.
24. Dagosta FCP, de Pinna M, Peres CA, Tagliacollo VA. 2021. Existing protected areas provide a poor safety-net for threatened Amazonian fish species. *Aquat Conserv*. 31:1167-1189.
25. Darriba D, Posada D, Kozlov AM, Stamatakis A, Morel B, Flouri T. 2020. ModelTest-NG: a new and scalable tool for the selection of DNA and protein evolutionary models. *Mol Biol Evol*. 37:291-294.
26. Davey JW, Hohenlohe PA, Etter PD, Boone JQ, Catchen JM, Blaxter ML. 2011. Genome-wide genetic marker discovery and genotyping using next-generation sequencing. *Nat Rev Genet*. 12:499-510.
27. Deon GA, Glugoski L, Vicari MR, Nogaroto V, Sassi FMC, Cioffi MB, Liehr T, Bertollo LAC, Moreira-Filho O. 2020. Highly Rearranged Karyotypes and

Multiple Sex Chromosome Systems in Armored Catfishes from the Genus *Harttia* (Teleostei, Siluriformes). *Genes*. 11:1366.

28. Deon GA, Glugoski L, Hatanaka T, Sassi FMC, Nogaroto V, Bertollo LAC, Liehr T, Al-Rikabi A, Moreira-Filho O, Cioffi MB, Vicari MR. 2022a. Evolutionary breakpoint regions and chromosomal remodeling in *Harttia* (Siluriformes: Loricariidae) species diversification. *Genet Mol Biol.* 45:e20210170.
29. Deon GA, Glugoski L, Sassi FMC, Hatanaka T, Nogaroto V, Bertollo LAC, Liehr T, Al-Rikabi A, Moreira-Filho O, Cioffi MB, Vicari MR. 2022b. Chromosomal Rearrangements and Origin of the Multiple XX/XY_1Y_2 Sex Chromosome System in *Harttia* Species (Siluriformes: Loricariidae). *Front Genet*. 13:877522.
30. Deon GA, dos Santos RZ, Sassi FMC, Moreira-Filho O, Vicari MR, Porto-Foresti F, Utsunomia R, Cioffi MB. The role of satellite DNAs in the chromosomal rearrangements and the evolution of the rare XY_1Y_2 sex system in *Harttia* (Siluriformes: Loricariidae). *J Hered*. 115:541-551.
31. Dobry J, Wapstra E, Stringer EJ, Gruber B, Deakin JE, Ezaz T. 2023. Widespread chromosomal rearrangements preceded genetic divergence in a monitor lizard, *Varanus acanthurus* (Varanidae). *Chromosome Res*. 31:9.
32. El Taher A, Ronco F, Matschiner M, Salzburger W, Böhne A. 2021. Dynamics of sex chromosome evolution in a rapid radiation of cichlid fishes. *Sci Adv*. 7:eabe8215.
33. Faber-Hammond JJ, Phillips RB, Brown KH. 2015. Comparative analysis of the shared sex-determination region (SDR) among salmonid fishes. *Genome Biol Evol.* 7:1972-1987.

34. Flouri T, Jiao X, Rannala B, Yang Z. 2018. Species tree inference with BPP using genomic sequences and the multispecies coalescent. *Mol Biol Evol.* 35:2585-2593.

35. Foll M, Gaggiotti O. 2008. A genome-scan method to identify selected loci appropriate for both dominant and codominant markers: a Bayesian perspective. *Genetics.* 180:977-993.

36. Fricke R, Eschmeyer WN, van der Laan R. 2025. Eschmeyer's Catalog of Fishes: Genera, Species, References. Available at http://researcharchive.calacademy.org/research/ichthyology/catalog/fishcatmain.asp. Last accessed August 02, 2025.

37. Furman BL, Metzger DC, Darolti I, Wright AE, Sandkam BA, Almeida P, Shu JJ, Mank JE. 2020. Sex chromosome evolution: so many exceptions to the rules. *Genome Biol Evol*. 12:750-763.

38. Gabilondo, A. R., Pérez, L. H., & Rodríguez, R. M. 2021. Hormonal and neuroendocrine control of reproductive function in teleost fish. *Rev Bionat*. 6:2122-2133.

39. Glick L, Mayrose I. 2014. ChromEvol: assessing the pattern of chromosome number evolution and the inference of polyploidy along a phylogeny. *Mol Biol Evol*. 31:1914-1922.

40. Glugoski L, Giuliano-Caetano L, Moreira-Filho O, Vicari MR, Nogaroto V. 2018. Co-located hAT transposable element and 5S rDNA in an interstitial telomeric sequence suggest the formation of Robertsonian fusion in armored catfish. *Gene*. 650:49-54.

41. Graves JAM. 2006. Sex chromosome specialization and degeneration in mammals. *Cell*. 124:901-914.

42. Graves JAM. 2016. Evolution of vertebrate sex chromosomes and dosage compensation. *Nat Rev Genet.* 17:33-46.

43. Gruber B, Unmack PJ, Berry OF, Georges A. 2018. dartr: An r package to facilitate analysis of SNP data generated from reduced representation genome sequencing. *Mol Ecol Resour.* 18:691-699.

44. Hayashi S, Abe T, Igawa T, Katsura Y, Kazama Y, Nozawa M. 2024. Sex chromosome cycle as a mechanism of stable sex determination. *J Biochem.* 176:81-95.

45. Hospodářská M, Mora P, Voleníková AC, Al-Rikabi A, Altmanová M, Simanovsky SA, Tolar N, Pavlica T, Janečková K, Štundlová J, et al. 2025. Multiple Origins of Sex Chromosomes in *Nothobranchius* Killifishes. *Mol Ecol*. 0:e70029.

46. Hubert N, Renno JF. 2006. Historical biogeography of South American freshwater fishes. *J Biogeogr.* 33:1414-1436.

47. Jaccoud D, Peng K, Feinstein D, Kilian A. 2001. Diversity arrays: a solid state technology for sequence information independent genotyping. *Nucleic Acids Res*. 29:e25.

48. Kabir A, Ieda R, Hosoya S, Fujikawa D, Atsumi K, Tajima S, Nozawa A, Koyama T, Hirase S, Nakamura O, et al. 2022. Repeated translocation of a supergene underlying rapid sex chromosome turnover in *Takifugu* pufferfish. *Proc Natl Acad Sci U S A*. 119:e2121469119.

49. Keating SE, Blumer M, Grismer LL, Lin A, Nielsen SV, Thura MK, Wood PL, Wuah ES, Gamble T. 2021. Sex chromosome turnover in bent-toed geckos (*Cyrtodactylus*). *Genes*. 12:116.

50. Kirschner P, Perez MF, Záveská E, Sanmartín I, Marquer L, Schlick-Steiner BC, Alvarez, the STEPPE Consortium, Steiner FM, Schönswetter P. 2022. Congruent evolutionary responses of European steppe biota to late Quaternary climate change. *Nat Comm*. 13:1921.
51. Kitano J, Peichel CL. 2012. Turnover of sex chromosomes and speciation in fishes. *Environ Biol Fishes*. 94:549-558.
52. Kitano J, Ross JA, Mori S, Kume M, Jones FC, Chan YF, Absher DM, Grimwood J, Schmutz J, Myers RM, et al. 2009. A role for a neo-sex chromosome in stickleback speciation. *Nature*. 461:1079-1083.
53. Knief U, Müller IA, Stryjewski KF, Metzler D, Sorenson M, Wolf JB. 2024. Evolution of chromosomal inversions across an avian radiation. *Mol Biol Evol.* 41:msae092.
54. Kottler VA, Schartl M. 2018. The colorful sex chromosomes of teleost fish. *Genes*. 9:233.
55. Kratochvíl L, Stöck M, Rovatsos M, Bullejos M, Herpin A, Jeffries DL, Peichel CL, Perrin N, Valenzuela N, Pokorná MJ. 2021. Expanding the classical paradigm: what we have learnt from vertebrates about sex chromosome evolution. *Philos Trans R Soc Lond B Biol Sci*. 376:20200097.
56. Krysanov E, Demidova T. 2018. Extensive karyotype variability of African fish genus *Nothobranchius* (Cyprinodontiformes). *Comp Cytogenet*. 12:387.
57. Kumar S, Suleski M, Craig JM, Kasprowicz AE, Sanderford M, Li M, Stecher G, Hedges SB. 2022. TimeTree 5: an expanded resource for species divergence times. *Mol Biol Evol.* 39:msac174.

58. Lambert MR, Skelly DK, Ezaz T. 2016. Sex-linked markers in the North American green frog (*Rana clamitans*) developed using DArTseq provide early insight into sex chromosome evolution. *BMC Genomics*. 17:844.
59. Lambert S, Voznica J, Hélène Morlon. 2023. Deep Learning from Phylogenies for Diversification Analyses. *Sys Biol.* 72:1262-1279.
60. Lande R, Seehausen O, van Alphen JJ. 2001. Mechanisms of rapid sympatric speciation by sex reversal and sexual selection in cichlid fish. *Genetica*. 112:435-443.
61. Landis MJ, Matzke NJ, Moore BR, Huelsenbeck J. 2013. Bayesian analysis of biogeography when the number of areas is large. *Sys Biol*. 62:789-804.
62. Li J, Zhou W, Wang Y, Niu C. 2018. The dual role of cGMP in oocyte maturation of zebrafish. *Biochem Biophys Res Commun*. 499:998-1003.
63. Lima FC, Ribeiro AC. 2011. Continental-scale tectonic controls of biogeography and ecology. *Historical biogeography of neotropical freshwater fishes*. University of California Press, Berkeley, 145-164.
64. Liu M, Song Y, Zhang S, Yu L, Yuan Z, Yang H, Zhang M, Zhou Z, Seim I, Liu S, et al. 2024. A chromosome-level genome of electric catfish (Malapterurus electricus) provided new insights into order Siluriformes evolution. *Mar Life Sci Technol*. 6:1–14
65. Londoño-Burbano A, Reis RE. 2021. A combined molecular and morphological phylogeny of the Loricariinae (Siluriformes: Loricariidae), with emphasis on the Harttiini and Farlowellini. *PloS One*. 16:e0247747.
66. Machado CB, Galetti Jr PM, Carnaval AC. 2018. Bayesian analyses detect a history of both vicariance and geodispersal in Neotropical freshwater fishes. *J Biogeogr*. 45:1313-1325.

67. Mackintosh A, Vila R, Laetsch DR, Hayward A, Martin SH, Lohse K. 2023. Chromosome fissions and fusions act as barriers to gene flow between *Brenthis* fritillary butterflies. *Mol Biol Evol.* 40:msad043.

68. Maddison WP, Midford PE, Otto SP. 2007. Estimating a binary character's effect on speciation and extinction. *Syst Biol*. 56:701-710.

69. Matzke NJ. 2018. BioGeoBEARS: BioGeography with Bayesian (and likelihood) Evolutionary Analysis with R Scripts. version 1.1.1, published on GitHub on November 6, 2018. DOI: http://dx.doi.org/10.5281/zenodo.1478250

70. McGaugh SE, Noor MA. 2012. Genomic impacts of chromosomal inversions in parapatric *Drosophila* species. *Philos Trans R Soc Lond B Biol Sci*. 367:422-429.

71. Melville J, Haines ML, Boysen K, Hodkinson L, Kilian A, Smith Date KL, Potvin DA, Parris KM. 2017. Identifying hybridization and admixture using SNPs: application of the DArTseq platform in phylogeographic research on vertebrates. *R Soc Open Sci.* 4:161061.

72. Mijangos JL, Gruber B, Berry O, Pacioni C, Georges A. 2022. dartR v2: An accessible genetic analysis platform for conservation, ecology and agriculture. *Methods Ecol Evol*. 13:2150-2158.

73. Mirarab S, Bayzid MS, Warnow T. 2016. Evaluating summary methods for multilocus species tree estimation in the presence of incomplete lineage sorting. *Sys Biol*. 65:366-380.

74. Montes C, Silva CA, Bayona GA, Villamil R, Stiles E, Rodriguez-Corcho AF, Beltrán-Triviño A, Lamus F, Muñoz-Granados MD, Pérez-Angel LC, et al. 2021. A middle to late Miocene trans-Andean portal: Geologic record in the Tatacoa Desert. *Front Earth Sci*. 8:587022.

75. Mujyambere V, Adomako K, Olympio OS. 2024. Effectiveness of DArTseq markers application in genetic diversity and population structure of indigenous chickens in Eastern Province of Rwanda. *BMC Genomics*. 25:193.

76. Muller HJ. 1918. Genetic variability, twin hybrids and constant hybrids, in a case of balanced lethal factors. *Genetics*. 3:422.

77. Nedoluzhko A, Sharko F, Tsygankova S, Boulygina E, Ibragimova A, Teslyuk A, Galindo-Villegas J, Rastorguev S. Genomic evidence supports the introgression between two sympatric stickleback species inhabiting the White Sea basin. *Heliyon*. 7:e06160.

78. Ohno S. 1966. Differentiation of the Primitive Sex Elements at the Expense of the Y or W, and the Conservation of the Original X or Z. In Sex Chromosomes and sex-linked genes (13-24). Berlin, Heidelberg: Springer Berlin Heidelberg.

79. Ortiz D, Pekár S, Bilat J, Alvarez N. 2021. Poor performance of DNA barcoding and the impact of RAD loci filtering on the species delimitation of an Iberian ant-eating spider. *Mol Phylogenet Evol.* 154:106997.

80. Oyakawa O, Fichberg I, Rapp-Py Daniel LH. Three new species of *Harttia* (Loricariidae: Loricariinae) from Serra do Cachimbo, rio Xingu basin, Pará, Northern Brazil. *Zootaxa*. 4387:75–90.

81. Palmer DH, Rogers TF, Dean R, Wright AE. 2019. How to identify sex chromosomes and their turnover. *Mol Ecol*. 28:4709-4724.

82. Paradis E, Schliep K. 2019. ape 5.0: an environment for modern phylogenetics and evolutionary analyses in R. *Bioinformatics*. 35:526-528.

83. Pennell MW, Kirkpatrick M, Otto SP, Vamosi JC, Peichel CL, Valenzuela N, Kitano J. 2015. Y fuse? Sex chromosome fusions in fishes and reptiles. *PLoS Genet*. 11:e1005237.

84. Pokorná M, Altmanová M, Kratochvíl L. 2014. Multiple sex chromosomes in the light of female meiotic drive in amniote vertebrates. *Chrom Res*. 22:35-44.

85. Potter S, Bragg JG, Blom MP, Deakin JE, Kirkpatrick M, Eldridge MD, Moritz C. 2017. Chromosomal speciation in the genomics era: disentangling phylogenetic evolution of rock-wallabies. *Front Genet.* 8:10.

86. Rambaut A. 2018. FigTree v1. 4.4. Available at https://github.com/rambaut/figtree/releases/tag/v1.4.4.

87. Rambaut A, Drummond AJ, Xie D, Baele G, Suchard MA. 2018. Posterior summarization in Bayesian phylogenetics using Tracer 1.7. *Syst Biol*, 67:901-904.

88. Rapp Py-Daniel LH. 1997. Unpublished data: Phylogeny of the Neotropical armored catfishes of the subfamily Loricariinae (Siluriformes: Loricariidae). Available at https://www.proquest.com/openview/8b63544fca6e7c4586db5dccff3e4e05/1?pq-origsite=gscholar&cbl=18750&diss=y.

89. Ree RH, Smith SA. 2008. Maximum likelihood inference of geographic range evolution by dispersal, local extinction, and cladogenesis. *Syst Biol*. 57:4-14.

90. Ree RH, Sanmartín I. 2018. Conceptual and statistical problems with the DEC+ J model of founder-event speciation and its comparison with DEC via model selection. *J Biogeogr*. 45:741-749.

91. Ronquist F. 1997. Dispersal-vicariance analysis: a new approach to the quantification of historical biogeography. *Syst Biol*, 46:195-203.

92. Rossetti DF, Valeriano MM. 2007. Evolution of the lowest amazon basin modeled from the integration of geological and SRTM topographic data. *Catena*. 70:253-265.

93. Roxo FF, Ochoa LE, Sabaj MH, Lujan NK, Covain R, Silva GSC, Melo BF, Albert JS, Chang J, Foresti F, et al. Phylogenomic reappraisal of the Neotropical catfish family Loricariidae (Teleostei: Siluriformes) using ultraconserved elements. *Mol Phylogenet Evol*. 135:148-165.

94. Sassi FMC, Deon GA, Moreira-Filho O, Vicari MR, Bertollo LAC, Liehr T, Oliveira EA, Cioffi MB. 2020. Multiple Sex Chromosomes and Evolutionary Relationships in Amazonian Catfishes: The Outstanding Model of the Genus *Harttia* (Siluriformes: Loricariidae). *Genes*. 11:1179.

95. Sassi FMC, Moreira-Filho O, Deon GA, Sember A, Bertollo LAC, Liehr T, Oliveira VCS, Viana PF, Feldberg E, Vicari MR, Cioffi MB. 2021. Adding New Pieces to the Puzzle of Karyotype Evolution in *Harttia* (Siluriformes, Loricariidae): Investigation of Amazonian Species*. Biology*. 10:922.

96. Sassi FMC, Sember A, Deon GA, Liehr T, Padutsch N, Oyakawa OT, Vicari MR, Bertollo LAC, Moreira-Filho O, Cioffi MB. 2023a. Homeology of sex chromosomes in Amazonian *Harttia* armored catfishes supports the X-fission hypothesis for the X_1X_2Y sex chromosome system origin. *Sci Rep.* 13:15756.

97. Sassi FMC, Deon GA, Sember A, Liehr T, Oyakawa OT, Moreira-Filho O, Bertollo LAC, Vicari MR, Cioffi MB. 2023b. Turnover of multiple sex chromosomes in Harttia catfish (Siluriformes, Loricariidae): a glimpse from whole chromosome painting. *Front Genet*. 14:1226222.

98. Sassi FMC, Cioffi MB, Moreira-Filho O. 2024. A state-of- art review of Loricariidae (Ostariophysi: Siluriformes) cytogenetics. *Neotrop Ichthyol*. 22:e240050.

99. Sassi FMC, Garrido-Ramos MA, Utsunomia R, dos Santos RZ, Ezaz T, Deon GA, Porto-Foresti F, Liehr T, Cioffi MB. Independent evolution of satellite DNA

sequences in homologous sex chromosomes of Neotropical armored catfish (*Harttia*). *Commun Biol*. 8:524.

100. Sember A, Nguyen P, Perez MF, Altmanová M, Ráb P, Cioffi MB. 2021. Multiple sex chromosomes in teleost fishes from a cytogenetic perspective: state of the art and future challenges. *Philos Trans R Soc Lond B Biol Sci*. 376:20200098.

101. Simmons MP, Gatesy J. 2021. Collapsing dubiously resolved gene-tree branches in phylogenomic coalescent analyses. *Mol Phylogenet Evol.* 158:107092.

102. Sopniewski J, Shams F, Scheele BC, Kefford BJ, Ezaz T. 2019. Identifying sex-linked markers in *Litoria aurea*: a novel approach to understanding sex chromosome evolution in an amphibian. *Sci Rep*. 9:16591.

103. Stamatakis A. 2014. RAxML version 8: a tool for phylogenetic analysis and post-analysis of large phylogenies. *Bioinformatics*. 30:1312-1313.

104. Štundlová J, Hospodářská M, Lukšíková K, Voleníková A, Pavlica T, Altmanová M, Richter A, Reichard Mm, Dalíkova M, Pelikánová Š, et al. 2022. Sex chromosome differentiation via changes in the Y chromosome repeat landscape in African annual killifishes *Nothobranchius furzeri* and *N. kadleci*. *Chrom Res*. 30:309-333.

105. Suchan T, Bataille CP, Reich MS, Toro-Delgado E, Vila R, Pierce NE, Talavera G. 2024. A trans-oceanic flight of over 4,200 km by painted lady butterflies. *Nature Commun*. 15:5205.

106. Tagliacollo VA, Roxo FF, Duke-Sylvester SM, Oliveira C, Albert JS. 2015. Biogeographical signature of river capture events in Amazonian lowlands. *J Biogeogr*. 42:2349-2362.

107. Tiley GP, Poelstra JW, Dos Reis M, Yang Z, Yoder AD. 2020. Molecular clocks without rocks: new solutions for old problems. *Trends Genet*. 36: 845-856.

108. Toups MA, Rodrigues N, Perrin N, Kirkpatrick M. 2019. A reciprocal translocation radically reshapes sex-linked inheritance in the common frog. *Mol Ecol.* 28:1877-1889.

109. Trudeau VL. 2022. Neuroendocrine control of reproduction in teleost fish: concepts and controversies. *Annu Rev Anim Biosci*. 10:107-130.

110. Van Doorn GS, Kirkpatrick M. 2007. Turnover of sex chromosomes induced by sexual conflict. *Nature*. 449:909-912.

111. Wang D, Li Y, Li M, Yang W, Ma X, Zhang L, Wang Y, Feng Y, Zhang Y, Zhou R, et al. 2022. Repeated turnovers keep sex chromosomes young in willows. *Genome Biol*. 23:200

112. Wang Y, Zhang RG, Hörandl E, Zhang ZX, Charlesworth D, He L. 2024. Evolution of sex-linked genes and the role of pericentromeric regions in sex chromosomes: insights from diploid willows. *Mol Biol Evol*. 41:msae235.

113. Warmerdam DO, Wolthuis RM. 2019. Keeping ribosomal DNA intact: a repeating challenge. *Chrom Res*, 27:57-72.

114. Wenzl P, Carling J, Kudrna D, Jaccoud D, Huttner E, Kleinhofs A, Kilian A. 2004. Diversity Arrays Technology (DArT) for whole-genome profiling of barley. *Proc Natl Acad Sci U S A*. 101:9915-9920.

115. White MJD. 1940. The origin and evolution of multiple sex-chromosome mechanisms. *J Genet.* 40:303-336.

116. Yang Z. 2015. The BPP program for species tree estimation and species delimitation. *Current Zool.* 61:854-865.

117. Yannic G, Basset P, Hausser J. 2009. Chromosomal rearrangements and gene flow over time in an inter-specific hybrid zone of the *Sorex araneus* group. *Heredity*. 102:616-625.

118. Yi X, Wang D, Reid K, Feng X, Löytynoja A, Merilä J. 2024. Sex chromosome turnover in hybridizing stickleback lineages. *Evol Lett*. 8:658-668.

119. Yoshida K, Kitano J. 2012. The contribution of female meiotic drive to the evolution of neo-sex chromosomes. *Evolution*. 66:3198-3208.

120. Zheng S, Tao H, Song Y, Li M, Yang H, Li J, Yan H, Sheraliev B, Tao W, Peng Z, et al. 2025. The origin, evolution, and translocation of sex chromosomes in *Silurus* catfish mediated by transposons. *BMC Biol*. 23:54.

121. Zhu Z, Younas L, Zhou Q. 2025. Evolution and regulation of animal sex chromosomes. *Nat Rev Genet*. 26:59-74.